

Positron Emission Tomographic Measurement of Blood-to-Brain and Blood-to-Tumor Transport of ^{82}Rb : The Effect of Dexamethasone and Whole-Brain Radiation Therapy

Jens O. Jarden, MD, Vijay Dhawan, PhD, Alexander Poltorak, PhD, Jerome B. Posner, MD, and David A. Rottenberg, MD

Unidirectional blood-to-brain and blood-to-tumor transport rate constants for rubidium 82 were determined using dynamic positron emission tomography in patients with primary or metastatic brain tumors. Regional influx rate constants (K_1) and plasma water volume (V_p) were estimated from the time course of blood and brain radioactivity following a bolus injection of tracer. Eight patients were studied before and 24 to 72 hours after treatment using pharmacological doses of dexamethasone, and 6 additional patients with metastatic brain tumors were studied before and within 60 to 90 minutes after 200- to 600-rad whole-brain radiation therapy. Steroid treatment was associated with a 9 to 48% decrease in tumor K_1 and a 21% mean decrease in tumor V_p . No consistent changes in K_1 or V_p were observed in control brain regions. Tumor K_1 and V_p did not increase in patients undergoing whole-brain radiation therapy, all of whom were taking dexamethasone at the time of study. These data suggest that corticosteroids decrease the permeability of tumor capillaries to small hydrophilic molecules (including those of some chemotherapeutic agents) and that steroid pretreatment prevents acute, and potentially dangerous, increases in tumor capillary permeability following cranial irradiation.

Jarden JO, Dhawan V, Poltorak A, Posner JB, Rottenberg DA: Positron emission tomographic measurement of blood-to-brain and blood-to-tumor transport of ^{82}Rb : the effect of dexamethasone and whole-brain radiation therapy. *Ann Neurol* 18:636-646, 1985

It is widely assumed that in patients with inflammatory and neoplastic cerebral lesions corticosteroids reduce brain swelling by decreasing brain/tumor capillary permeability to crystalloids and colloids. In human subjects, short-term corticosteroid treatment has been shown to diminish computed tomographic (CT) contrast enhancement [8, 14, 36, 39], and in experimental animals, steroids decrease brain uptake of intraarterially administered methotrexate following alteration of the blood-brain barrier (BBB) [29]. Positron emission tomographic (PET) measurements of regional cerebral blood flow (rCBF) and blood volume (rCBV) in patients with brain tumors and perifocal edema before and several days after dexamethasone treatment suggest that steroids have an "immediate diffuse effect" on the cerebral vasculature [24]. However, the extent to

which corticosteroids modulate the blood-to-brain transport of different ionic and molecular species and the basis for their anti-edema effect have not been elucidated.

The acute and chronic effects of whole-brain radiation therapy (WBRT) on the central nervous system are well known, although their pathogenesis remains a subject of continuing controversy [34]. An infrequently diagnosed complication of WBRT, radiation-induced cerebral edema, may be responsible for the increased morbidity and mortality associated with "rapid-course" treatment protocols incorporating high rad doses, and for the increase in ventricular cerebrospinal fluid (CSF) pressure after WBRT reported by Young and associates [43]. Using [^{14}C]α-aminoisobutyric acid and quantitative autoradiography,

From the Department of Neurology, Memorial Sloan-Kettering Cancer Center and Cornell University Medical College, New York, NY 10021.

Received Jan 18, 1985, and in revised form Apr 24. Accepted for publication Apr 24, 1985.

Address reprint requests to Dr Rottenberg, Memorial Sloan-Kettering Cancer Center, Department of Neurology, 1275 York Ave, New York, NY 10021.

Table 1. Summary of ^{82}Rb /PET Studies in Patients Undergoing Whole-Brain Radiation Therapy

| Patient No. | Sex/Age (yr) | Diagnosis ^a | Steroids (mg) ^b | RT Protocol (Rx) ^c | ^{82}Rb /PET Protocol ^d | | |
|-------------|--------------|------------------------|----------------------------|---------------------------------|---|----------|-----------------------------|
| | | | | | Pre-Rx | Post-Rx | Interval (min) ^e |
| 1 | M/23 | Ca testis | 16 | 200 rad × 10 (2) | Bolus | Bolus/CI | 59 |
| 2 | M/57 | Ca lung | 16 | 300 rad × 10 (2) | Bolus | Bolus/CI | 85 |
| 3 | M/55 | Ca lung | 16 | 600 rad × 3 (2), 400 rad × 3 | Bolus | Bolus | 60 |
| 4 | F/44 | Ca breast | 4 | 300 rad × 10 (3) | Bolus | Bolus/CI | 65 |
| 5 | M/69 | Mesothelioma | 16 | 300 rad × 10 (2) | Bolus | Bolus/CI | 90 |
| 6 | M/42 | Ca lung | 16 | 300 rad × 10 (3) | CI | CI | 75 |

^aAll patients had parenchymal brain metastases.

^bDaily oral dose of dexamethasone.

^cFractionation scheme (treatment number at time of study).

^dAdministered intravenously.

^eInterval between whole-brain radiation therapy (WBRT) and post-WBRT ^{82}Rb /PET scan.

PET = positron emission tomography; M = male; F = female; Ca = cancer; RT = radiation therapy; Rx = treatment; CI = constant infusion.

Caveness [6] demonstrated focal increases in BBB permeability in monkeys weeks to months after single high-dose brain irradiation. No acute experiments with α -aminoisobutyric acid were performed, and therefore the time course of the observed BBB lesions was not determined.

Intravenously administered rubidium (Rb), a potassium analogue, is excluded from the brain by the normal BBB. Previous studies have demonstrated the potential of ^{82}Rb (half-life, 76 sec) and PET for imaging regions of BBB disruption [5, 40–42]. Gallium 68 (^{68}Ga) (half-life, 68 min) in the form of [^{68}Ga]ethylenediaminetetraacetate has also been used with PET to quantitate the effects of brain tumors and hyperosmotic intracarotid infusions on BBB permeability [4, 15, 22]; however, the long isotopic half-life of ^{68}Ga relative to that of ^{82}Rb results in a higher absorbed dose per administered millicurie, longer PET imaging times, and longer delays between repeat or “before-and-after” studies, which constitute practical disadvantages for clinical studies.

In order to quantitate the effects of corticosteroids on BBB permeability, 9 patients with primary or metastatic brain tumors were studied with ^{82}Rb PET immediately before and 24 to 72 hours after dexamethasone treatment. Six additional patients with metastatic brain tumors were studied immediately before and 60 to 90 minutes after WBRT in an effort to quantitate the early effects of ionizing radiation on the blood-brain and blood-tumor barriers; patients receiving low-dose and high-dose fractions were included in order to study the effect of increasing rad dose on brain ^{82}Rb uptake.

Methods

Eight in-patients from Memorial Hospital who had primary (3 patients) or metastatic (5 patients) brain tumors were

studied before and 24 hours after the start of dexamethasone treatment; one additional patient with a metastatic brain tumor was studied before and 72 hours after the start of treatment. All patients received 100 mg of dexamethasone intravenously immediately after their first PET scan and 24 mg every 6 hours thereafter; no patient had received prior corticosteroids or other anti-edema therapy. A 24-hour treatment period was selected because clinical improvement is usually apparent within 6 to 12 hours after a 100-mg intravenous dose of dexamethasone. Six additional in-patients with metastatic brain tumors were studied immediately before and approximately 1 hour after 200-, 300-, or 600-rad WBRT (Table 1); all 6 patients were taking dexamethasone (4 to 16 mg/day) at the time of study. The choice of 1 hour was dictated by the fact that patients frequently complain of headache or somnolence within 1 to 2 hours after WBRT. Protocols for the dexamethasone and WBRT studies were approved by the Institutional Review Board of Memorial Hospital, and informed consent was obtained from each patient or his or her next of kin. All patients had transmission CT or nuclear magnetic resonance scan evidence of parenchymal brain lesions.

Approximately 60 to 120 mCi of ^{82}Rb , eluted from a Squibb $^{82}\text{Sr}/^{82}\text{Rb}$ generator (E. R. Squibb and Sons, New Brunswick, NJ) [12], in normal saline was injected as an intravenous bolus (50 ml/min × 2 min) or infused at a constant rate (15 ml/min × 7 min) through a 0.22- μ Millipore filter (Fig 1). The infusion apparatus consisted of a Harvard pump, two 60-ml sterile disposable syringes, and sterile plastic intravenous tubing and connectors.

Serial (7 × 60 sec or 10 × 30 sec, 2 × 60 sec) PET images were acquired for 7 minutes using the Cyclotron Corporation PC 4600 Positron Camera [20]. One-milliliter radial arterial blood samples were collected at 9-second intervals during the period of PET data acquisition by means of a high-speed peristaltic pump (Ole Dich, Copenhagen) and counted immediately in a well scintillation detector. Appropriate corrections were made for delayed arrival of intravenously injected isotope at the radial arterial sampling site, pump delay/“smearing” [33], and decay during the period of

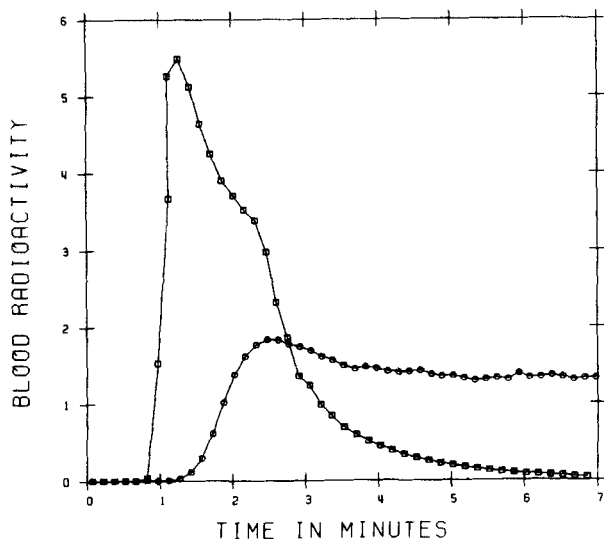


Fig 1. Time course of blood ^{82}Rb activity following bolus injection (squares) or continuous infusion (circles) of tracer from a Squibb $^{82}\text{Sr}/^{82}\text{Rb}$ generator. Blood activity in arbitrary units is plotted as a function of time.

measurement. A description of our technique for radial arterial catheterization is provided elsewhere [35]. Accurate patient repositioning was facilitated by a custom-molded polyurethane headholder-immobilizer [21] and crossed Gammex lasers. A transmission scan obtained before the pretreatment emission study served to confirm the anatomical level of section and to correct the before-and-after emission scans for tissue attenuation.

Region-of-interest (ROI) analysis was performed on 128×128 PET reconstructions, which were appropriately corrected for isotopic decay, random coincidences, tissue attenuation, and electronic deadtime. Whenever possible, large (greater than 2 cm in diameter) circular ROIs were selected within homogeneous brain/tumor regions in order to maximize recovery coefficients [27]. In order to minimize the effects of volume averaging, we attempted whenever possible to extract ROI data from the middle slice of three contiguous 1-cm slices containing tumor tissue. Control data for "normal" brain tissue were taken from a mirror ROI in the contralateral hemisphere. Values for the influx rate constant (K_1), the efflux rate constant (k_2), and plasma water volume (V_p) were obtained from $^{82}\text{Rb}/\text{PET}$ ROI and blood data and Equation 3, which was solved by a nonlinear least-squares regression algorithm.

Because of the high correlation between "before" and "after" values within patients (both for K_1 and V_p) and the wide range of values across patients, Student's t test was applied to the percent change in K_1 and V_p .

Rubidium Uptake in Red Blood Cells

Because of a suggestion in the literature that Rb is rapidly taken up into red blood cells (RBCs) after intravascular injection [38, 44], we determined the time course of Rb uptake into RBCs following an intravenous bolus injection of

^{82}Rb . For these experiments, which were performed in volunteer subjects, we administered approximately 20 mCi of ^{82}Rb intravenously according to the same infusion protocol adopted for $^{82}\text{Rb}/\text{PET}$ studies, and collected arterial blood from a radial arterial catheter at 9-second intervals. Every seventh blood sample was collected in a tared microcentrifuge tube, weighed, and counted for 6 seconds, then spun in a Beckman Microfuge B at 8,700 g for 15 seconds; 0.3 to 0.4 ml of the supernatant plasma was then pipetted rapidly into clean tared microcentrifuge vials, weighed, and counted as described above. Measured blood and plasma ^{82}Rb radioactivity, decay-corrected to the start of infusion, and the arterial hematocrit were used to compute the plasma-water-to-whole-blood-water ratio (PWR) for ^{82}Rb as a function of time; these data were fit to the function $\text{PWR} = a + bt$ (where a is the intercept with the Y axis and b is the slope of the line, and t is time after ^{82}Rb injection) and used to correct whole-blood measurements of ^{82}Rb radioactivity for RBC uptake. RBC and plasma water content were assumed to be 0.721 and 0.927 ml/gm, respectively [30]. For $^{82}\text{Rb}/\text{PET}$ patient studies, measured whole-blood ^{82}Rb concentrations were multiplied by the appropriate PWR in order to calculate plasma water ^{82}Rb concentration (C_p , see the following section).

Theory

A simple two-compartment model adequately describes the passive exchange of ^{82}Rb between arterial plasma and brain tissue (Fig 2). This exchange can be described mathematically by the following equations:

$$dA_f(t)/dt = K_1 C_p(t) - k_2 A_f(t) \quad \text{Eq 1}$$

$$A_m(t) = A_f(t) + V_p C_p(t) \quad \text{Eq 2}$$

where $A_f(t)$ is the ^{82}Rb concentration in extravascular brain tissue ($\mu\text{Ci}/\text{gm}$), $A_m(t)$ is the ^{82}Rb concentration in brain tissue ($\mu\text{Ci}/\text{gm}$), i.e., including intravascular label, and $C_p(t)$ is the instantaneous plasma ^{82}Rb concentration ($\mu\text{Ci}/\text{ml}$); K_1 is given in milliliters per minute per gram, k_2 is given as min^{-1} , and V_p is given in milliliters per gram. The use of V_p in Equation 2 assumes that label (^{82}Rb) is confined to the plasma space, which is probably not the case at the end of a 7-minute study (to be discussed later).

These relationships permit the estimation of K_1 , k_2 , and V_p from PET ROI data and the time course of blood ^{82}Rb activity:

$$A_m = \int_{T_1}^{T_2} A_m(t) dt = K_1 \int_{T_1}^{T_2} e^{-k_2 t} \int_0^t C_p(u) e^{k_2 u} du dt + \int_{T_1}^{T_2} V_p C_p(t) dt \quad \text{Eq 3}$$

where T_1 and T_2 are scan beginning and end times. An analysis of Equation 3 using computer simulations was performed in order to estimate the errors associated with \hat{K}_1 , \hat{k}_2 , and \hat{V}_p for both bolus and constant infusion protocols (see Appendix). The error in \hat{K}_1 varies from approximately 5 to 35% for $0.1 < K_1 < 0.001$, and the error in \hat{V}_p is less than 6% for $0.03 < V_p < 0.08$.

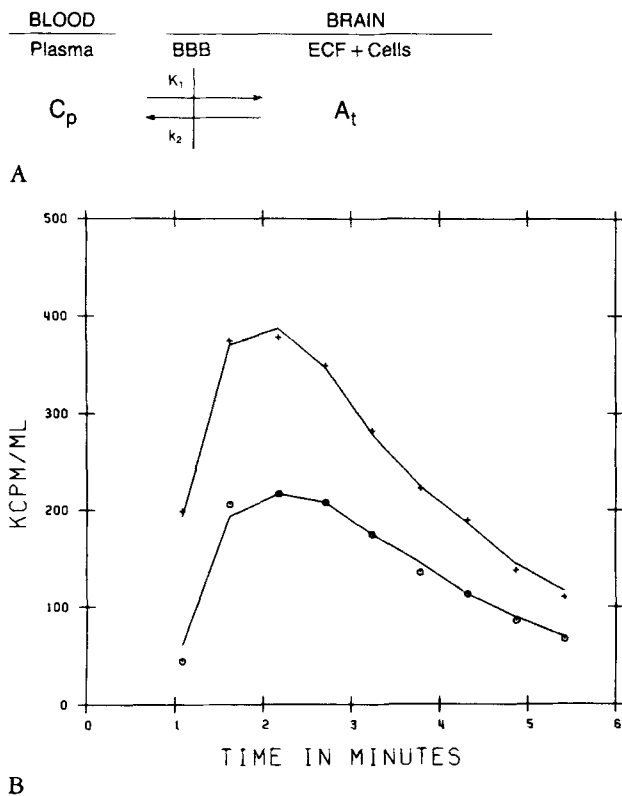


Fig 2. (A) Two-compartment model of the blood-to-brain transport of ^{82}Rb . C_p is plasma ^{82}Rb concentration ($\mu\text{Ci/ml}$), A_t is extravascular brain tissue ^{82}Rb concentration ($\mu\text{Ci/gm}$), and K_1 (ml/min/gm) and k_2 (min^{-1}) are influx and efflux rate constants, respectively. (ECF = extravascular fluid; BBB = blood-brain barrier.) (B) Relationship between the non-decay-corrected region-of-interest ROI data for two metastatic tumors (symbols) and corresponding plots derived from fitted model parameters and Equation 3. Radioactivity concentration (Kcpm/ml) is plotted versus time in minutes.

Results

Pre- and posttreatment ^{82}Rb /PET studies are illustrated in Figure 3, which emphasizes that the same tumor and contralateral control regions were analyzed on before-and-after scan sequences. Derived blood-to-brain and blood-to-tumor transfer constants and tissue plasma water volumes for Rb for 8 patients with large primary or metastatic tumors are presented in Table 2. One patient with an oligodendroglioma was not included in the table, as tumor ^{82}Rb concentration never exceeded that of contralateral brain tissue; his CT scan was not enhanced by iodinated contrast material. The mean decrease in tumor K_1 and V_p after dexamethasone treatment was highly significant. In view of the large uncertainty (greater than 70%) associated with estimates of k_2 (see Appendix), no conclusions could be drawn about the effect of dexamethasone on Rb efflux.

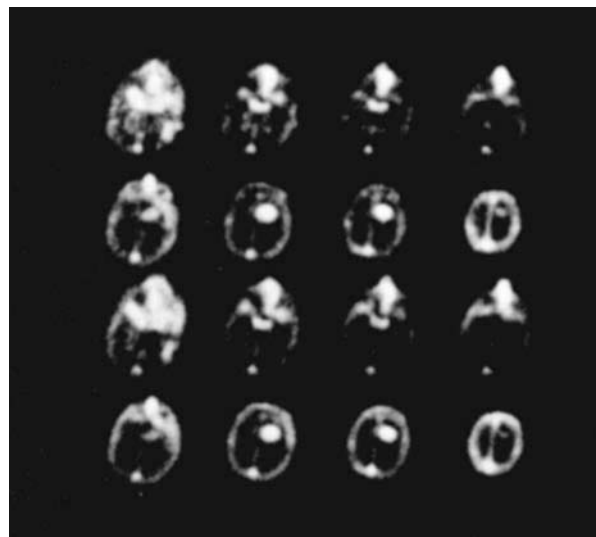


Fig 3. Contiguous 1-cm ^{82}Rb /PET (positron emission tomographic) brain slices before (upper two rows) and 24 hours after (lower two rows) dexamethasone treatment. The cerebral blood pool and a large right frontal metastasis are visible in these composite 7-minute images, which illustrate the repositioning accuracy achievable using a custom-molded headholder-immobilizer and crossed Gammex lasers.

Blood-to-brain and blood-to-tumor transfer constants and tissue plasma volume for 6 patients before and after WBRT are summarized in Table 3. There was no significant difference between pre- and post-treatment tumor K_1 values. V_p increased after WBRT in 5 of 6 tumors and in 4 of 6 control regions, but this increase was of borderline significance.

The distribution of ^{82}Rb between RBCs and plasma following bolus injection, expressed as (cps/ml of plasma water)/(cps/ml of whole-blood water) as a function of time, is defined by the data in Table 4 and Figure 4. Because of scatter in the experimental data, we did not correct the ratios for arterial hematocrit. The least-squares regression line, $\text{PWR} = 1.53 - 0.069t$, was used to correct whole-body radioactivity measurements for ^{82}Rb sequestered in RBCs.

The effect of ROI size on derived estimates of K_1 , k_2 , and V_p is illustrated in Figure 5 and Table 5 with reference to a metastatic tumor: concentrically decreasing the ROI area from 3.7 to 0.8 cm^2 resulted in an 11% increase in K_1 , a 14% decrease in k_2 , and a 23% increase in V_p .

Discussion

^{82}Rb , a short-lived positron-emitting analogue of potassium, is an ideal tracer for studies of BBB permeability. The absorbed dose per administered millicurie is low relative to fluorine 18, ^{68}Ga , or carbon 11, and short serial high-count-rate PET studies can be per-

Table 2. Derived Blood-to-Brain and Blood-to-Tumor Transfer Constants and Tissue Plasma Water Volume

| Patient No./ Tumor Type ^a | ROI Size (cm ²) | Before Steroids ^b | | After Steroids ^b | | % Change | |
|---|-----------------------------------|------------------------------|----------------|-----------------------------|----------------|------------------|------------------|
| | | K ₁ | V _p | K ₁ | V _p | K ₁ | V _p |
| 1/medulloblastoma | | | | | | | |
| Tumor ROI | 3.4 | 5.3E-2 | 0.060 | 4.8E-2 | 0.061 | -9 | +2 |
| Control ROI | 3.9 | 4.0E-3 | 0.039 | 5.0E-3 | 0.037 | +25 | -5 |
| 2/glioblastoma | | | | | | | |
| Tumor ROI | 1.3 | 1.2E-2 | 0.035 | 6.7E-3 | 0.029 | -44 | -17 |
| Control ROI | 8.4 | 1.4E-3 | 0.022 | 1.4E-3 | 0.018 | 0 | -2 |
| 3/nasopharyngeal Ca | | | | | | | |
| Tumor ROI | 7.6 | 5.5E-2 | 0.037 | 4.1E-2 | 0.022 | -25 | -41 |
| Control ROI | 7.0 | 4.0E-3 | 0.029 | 2.8E-3 | 0.027 | -30 | -7 |
| 4/lung Ca | | | | | | | |
| Tumor ROI | 3.2 | 5.6E-2 | 0.063 | 2.9E-2 | 0.037 | -48 | -41 |
| Control ROI | 8.3 | 7.5E-3 | 0.040 | 5.5E-3 | 0.043 | -27 | +8 |
| 5 ovarian Ca | | | | | | | |
| Tumor ROI | 2.5 | 7.2E-2 | 0.038 | 4.3E-2 | 0.027 | -40 | -29 |
| Control ROI | 9.1 | 2.4E-3 | 0.015 | 3.5E-3 | 0.012 | +46 | -20 |
| 6/lung Ca | | | | | | | |
| Tumor ROI | 2.8 | 8.2E-2 | 0.094 | 7.3E-2 | 0.087 | -11 | -7 |
| Control ROI | 9.1 | 1.5E-3 | 0.023 | 1.2E-3 | 0.026 | -20 | +13 |
| 7/bladder Ca | | | | | | | |
| Tumor ROI | 3.7 | 2.1E-2 | 0.027 | 1.6E-2 | 0.018 | -24 | -33 |
| Control ROI | 13.2 | 7.1E-3 | 0.031 | 7.4E-3 | 0.030 | +4 | -3 |
| 8/melanoma | | | | | | | |
| Tumor ROI | 1.7 | 9.4E-2 | 0.107 | 6.0E-2 | 0.085 | -36 | -21 |
| Control ROI | 9.6 | 7.2E-3 | 0.031 | 7.4E-3 | 0.033 | +3 | +6 |
| Mean Tumor | | 5.6E-2 | 0.058 | 4.0E-2 | 0.046 | -29 ^c | -21 ^d |
| Mean Control | | 4.4E-3 | 0.029 | 4.2E-3 | 0.028 | -5 | -3 |

N.B. ⁸²Rb was administered as an intravenous bolus. Stable efflux rate constant (*k*₂) values could not be obtained with the 10 × 30 sec, 2 × 60 sec scanning protocol used for these studies.

^aPatients had either primary or metastatic brain tumors.

^bFor tumor and control ROIs, K₁ (in exponential notation) is expressed as ml/min/gm and V_p as ml/gm. Dexamethasone dosage schedule: 100-mg intravenous bolus, then 24 mg every 6 hours for 24 hours or 72 hours (Patient 7).

^ct = 5.66; p < 0.001.

^dt = 4.07; p < 0.01.

K₁ = the influx rate constant (in exponential notation); V_p = tissue plasma water volume; ROI = region of interest; Ca = cancer.

formed safely. For before-and-after studies, only 6 to 10 minutes are required for isotopic decay, and therefore corrections for residual radioactivity are not required. Ionic ⁸²Rb (specific activity, 1.5 × 10⁵ Ci/μM) was eluted with normal saline from a portable Squibb generator [12] and infused directly into patients by means of a Harvard pump. The radiation absorbed dose for ⁸²Rb has been estimated by Kearfott [19]: per administered millicurie, the kidney (critical organ), heart, and total body receive 19, 13, and 1.6 mrad, respectively. Thus, an equivalent bolus of 100 mCi results in a kidney dose of approximately 2 rad.

The data in Table 4 suggest that ⁸²Rb rapidly enters RBCs and that a time-dependent correction for RBC ⁸²Rb concentration should be applied to whole-blood measurements of ⁸²Rb radioactivity. It should be noted that Lammertsma and associates [23] assumed no ⁸²Rb uptake by RBCs, since whole-blood ⁸²Rb concentra-

tions calculated from plasma concentrations and the peripheral hematocrit were only 3% lower than the measured whole-blood ⁸²Rb concentrations. We have no explanation for these discrepant results.

Like potassium, intravenously administered Rb is excluded from the brain by the normal BBB. When, however, BBB permeability is increased, e.g., within and around primary and metastatic brain tumors, tissue uptake is increased. This increased uptake is primarily attributable to increased (ionic) diffusion, although other mechanisms may also be involved. ⁸²Rb in arterial plasma water crosses the BBB (and/or BBB complex) to enter brain tissue water, i.e., extracellular fluid (ECF) and intracellular fluid (ICF) water. Astrocytes and other perithelial cells may actively accumulate tracer that has traversed the capillary endothelial barrier [16], and recent evidence suggests that Rb is transported from brain extracellular space into endothelial

Table 3. Derived Blood-to-Brain and Blood-to-Tumor Transfer Constants and Tissue Plasma Water Volume

| Patient No. ^a | ROI Size (cm ²) | Before WBRT ^b | | | After WBRT ^b | | |
|--------------------------|-----------------------------|--------------------------|------------------|----------------|-------------------------|------------------|----------------|
| | | K ₁ | k ₂ | V _p | K ₁ | k ₂ | V _p |
| Patient 1 | | | | | | | |
| Tumor ROI | 2.1 | 9.0E-2 | 7.2E-2 | 0.095 | 9.0E-2 | 8.3E-2 | 0.083 |
| Control ROI | 2.1 | 5.8E-3 | 4.1E-3 | 0.026 | 3.1E-3 | 7.1E-3 | 0.030 |
| Patient 2 | | | | | | | |
| Tumor ROI | 2.7 | 5.3E-2 | 2.6E-2 | 0.037 | 6.4E-2 | 1.1E-2 | 0.043 |
| Control ROI | 3.0 | 5.5E-3 | 4.1E-3 | 0.045 | 5.1E-3 | 3.1E-3 | 0.055 |
| Patient 3 | | | | | | | |
| Tumor ROI | 2.1 | 5.0E-2 | 1.0E-1 | 0.045 | 6.6E-2 | 5.9E-2 | 0.059 |
| Control ROI | 3.8 | 1.2E-3 | 9.7E-3 | 0.025 | 1.7E-3 | 8.4E-3 | 0.025 |
| Patient 4 | | | | | | | |
| Tumor ROI | 2.1 | 1.1E-1 | 1.0E-1 | 0.057 | 9.4E-2 | 6.7E-2 | 0.076 |
| Control ROI | 2.1 | 2.0E-3 | 8.7E-3 | 0.013 | 1.1E-3 | 7.6E-3 | 0.018 |
| Patient 5 | | | | | | | |
| Tumor ROI | 3.1 | 1.3E-1 | 7.4E-2 | 0.031 | 1.1E-1 | 3.4E-2 | 0.042 |
| Control ROI | 2.1 | 1.7E-3 | 8.9E-3 | 0.022 | 2.7E-3 | 8.1E-3 | 0.019 |
| Patient 6 | | | | | | | |
| Tumor ROI | 1.3 | 4.3E-2 | ... ^c | 0.040 | 3.3E-2 | ... ^c | 0.060 |
| Control ROI | 9.0 | 4.9E-3 | 6.2E-3 | 0.011 | 5.2E-4 | 1.1E-2 | 0.020 |

^a⁸²Rb administered as an intravenous bolus (Patients 1–5) or by continuous intravenous infusion (Patient 6).

^bK₁ (in exponential notation; ml/min/gm); k₂ (in exponential notation; min⁻¹); V_p (min⁻¹).

^cToo small to determine accurately.

WBRT = whole-brain radiation therapy; K₁ = the influx rate constant; k₂ = the efflux rate constant; V_p = tissue plasma water volume; ROI = region of interest.

Table 4. Time Course of ⁸²Rb Exchange between Plasma Water and Red Blood Cell Water following Bolus Intravenous Injection^a

| Patient No. | Hct | Time after Start of Bolus Injection ^b | | | | | |
|-------------|-----|--|------|------|------|------|------|
| | | 1 | 2 | 3 | 4 | 5 | 6 |
| 1 | 29 | ... | 1.22 | 1.23 | 1.46 | 1.10 | 1.04 |
| 2 | 34 | 1.27 | 1.54 | 1.23 | 1.27 | 1.19 | 1.03 |
| 3 | 43 | 1.48 | 1.56 | 1.40 | 1.24 | 1.27 | 1.16 |
| 4 | 47 | 1.70 | 1.38 | 1.36 | 1.38 | 1.25 | 1.37 |
| 5 | 48 | ... | 1.07 | 1.32 | 1.25 | 1.14 | 0.83 |
| Mean | | 1.48 | 1.35 | 1.31 | 1.32 | 1.19 | 1.09 |

^aExpressed as the ratio of [⁸²Rb]/ml of plasma water to [⁸²Rb]/ml of whole-blood water. Neglecting the difference in water content between red blood cells and plasma, for a hematocrit (Hct) of 40, this ratio would be expected to vary from 1.67 (⁸²Rb only within plasma water) to 1.00 (⁸²Rb distributed equally between red blood cells and plasma water).

^bTime in minutes.

cell cytoplasm by a (Na⁺ + K⁺)-adenosine triphosphatase ([Na⁺ + K⁺]-ATPase) located in the abluminal membrane of brain capillary endothelium [2, 9, 10]. The simplified two-compartment model illustrated in Figure 2A does not specifically account for the passive exchange of Rb between ECF and ICF water, nor does it describe the active accumulation of tracer by astrocytes and/or other perithelial cells (see

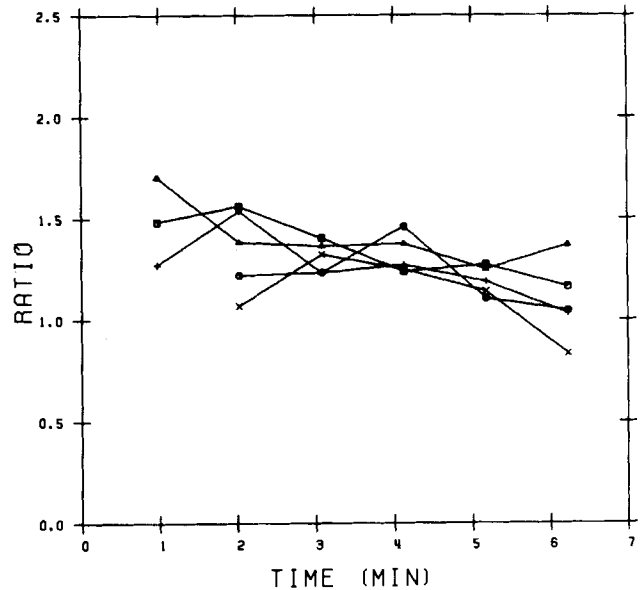


Fig 4. Uptake of ⁸²Rb into red blood cells (RBCs) following intravenous bolus injection. The ratio of [⁸²Rb]/ml of plasma water to [⁸²Rb]/ml of whole-blood water is plotted as a function of time for 5 patient studies (cf. Table 4).

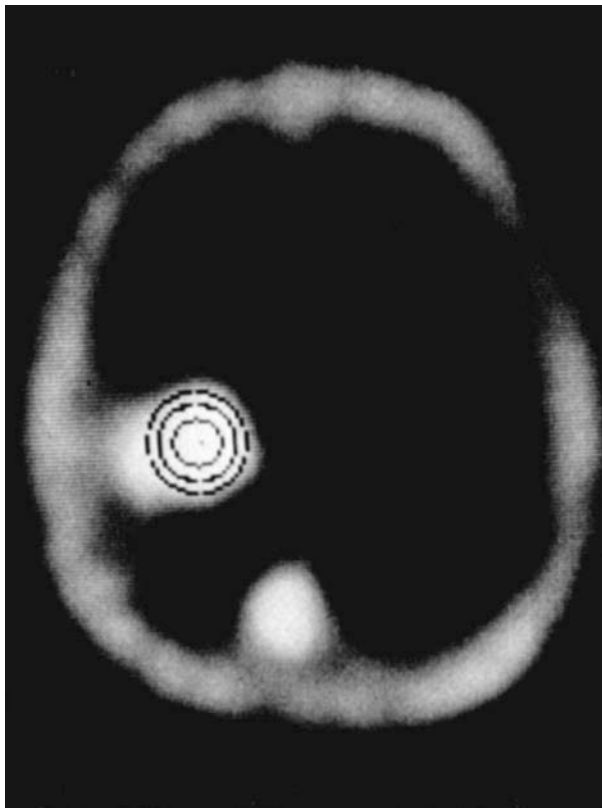


Fig 5. Concentric 3.7-, 1.9-, and 0.8-cm² regions of interest superimposed on a left frontoparietal metastasis from carcinoma of the testis. Calculated rate constants and distribution volumes for ⁸²Rb are summarized in Table 5.

Appendix). In spite of the above-mentioned limitations, our data suggest that a two-compartment model provides physiologically relevant information about blood-to-brain and blood-to-tumor transport of ⁸²Rb. A similar two-compartment tracer kinetic model has recently been proposed by Hawkins and associates [15] for evaluating BBB permeability in human brain tumors using ⁶⁸Ga-labeled EDTA and PET.

The use of ⁸²Rb for PET measurements of BBB permeability was pioneered by Yano and colleagues [40], who developed a precision flow-controlled ⁸²Rb generator for bolus or constant-infusion studies. Yen and Budinger [41] and, later, Yen's group [42] demonstrated the potential of ⁸²Rb/PET for clinical investigation; their ⁸²Rb/PET images of metastatic brain tumors emphasize the high ratio of tumor-to-brain activity achievable with this technique. Yen and associates [42] compared the uptake of ⁸²Rb (using PET) to CT contrast enhancement in 8 patients with primary or metastatic brain tumors; CT contrast enhancement was demonstrated in 5 of the 8 patients, whereas ⁸²Rb/PET studies were abnormal in 6 of 8. The authors concluded that tumor uptake of ⁸²Rb in patients with negative contrast-enhanced CT scans reflected a larger

Table 5. Effect of Region-of-Interest Size on Calculated Transport Rate Constants and Distribution Volumes for ⁸²Rb

| ROI size (cm ²) ^a | K ₁ ^b | k ₂ ^b | V _p |
|--|-----------------------------|-----------------------------|----------------|
| 3.7 | 7.1E-2 | 1.0E-1 | 0.056 |
| 1.9 | 7.7E-2 | 9.9E-2 | 0.062 |
| 0.8 | 7.9E-2 | 8.6E-2 | 0.069 |

^aSee Figure 5.

^bIn exponential notation.

ROI = region of interest.

extravascular distribution space for ⁸²Rb than for iodinated contrast material or a greater increase in BBB permeability to smaller tracers.

Brooks and associates [5] used ⁸²Rb/PET and a steady-state model involving measurement of rCBF and rCBV to obtain quantitative measurements of regional Rb extraction in normal subjects and in patients suffering from a variety of neurological conditions. One patient with a solitary cerebral metastasis was studied before and after treatment with dexamethasone (4 mg orally four times a day for 48 hours) and then 2 weeks later following 2000-rad WBRT. Dexamethasone treatment had little effect on Rb extraction by tumor or contralateral cerebral tissue; however, following radiotherapy the Rb permeability-surface area (PS) product of the tumor more than doubled, whereas that of contralateral brain tissue remained unchanged. Brooks's group compared Rb extraction by tumor tissue and contralateral brain in treated (WBRT) versus untreated patients with primary or metastatic brain tumors; treated patients were studied between 1 and 6 months "after courses of radiotherapy." They concluded that there was no significant difference in Rb extraction by tumor or contralateral brain tissue between treated and untreated groups. The extent to which simultaneous treatment with corticosteroids may have influenced these results was not discussed.

Parameter Estimation

Although solutions for k_2 were associated with large uncertainties (see Appendix), realistic values of K_1 and V_p were obtained for tumor and control brain ROIs (see Tables 2, 3). A formal error analysis of our method (see Appendix) suggests that for a 7-minute study the error in \hat{K}_1 is similar for both the continuous-infusion and the bolus-injection protocols. For the bolus-injection technique, the error in tumor \hat{K}_1 varies from -5 to +35% for $0.1 < K_1 < 0.001$. The error in \hat{V}_p is less than 6% for $0.1 < K_1 < 0.0001$.

The solution to Equation 3 requires a straightforward, if rather cumbersome, nonlinear regression. Linearization of the problem involves simplifying assumptions but allows for much more rapid solutions

and yields essentially the same result as the nonlinear solution (see Appendix). The consistency of our results for both tumor and control regions suggests that repositioning errors, volume averaging, and variation in recovery coefficients do not invalidate our conclusions. Our control K_1 values are similar to the capillary transfer constants obtained by Blasberg and associates [3] in rats and rhesus monkeys using [^{14}C] α -aminoisobutyric acid and quantitative autoradiography, and our tumor K_1 values are comparable to those obtained by Groothuis and colleagues [13] for canine gliomas using meglumine iothalamate and dynamic transmission CT but are, in general, greater than those reported by Hawkins and co-workers [15] for human brain tumors using [^{68}Ga]EDTA/PET. It is difficult, however, to compare our tumor values with those of Hawkins's group, since the latter researchers do not provide any information regarding the treatment status (e.g., WBRT, corticosteroids) of their subjects. Most significantly, K_1 s calculated from the Rb extraction and rCBF data of Brooks and colleagues [5] for enhancing tumors and contralateral brain are virtually identical to the before-steroids mean tumor and mean control values in Table 2. This is reassuring, in view of the methodological and conceptual differences between our bolus ^{82}Rb /dynamic PET method and the steady-state technique employed by Brooks's group.

Regional influx constants can be related to the regional PS product:

$$PS = -FV_f \cdot \ln(1 - K/FV_f) \quad \text{Eq 4}$$

where F is the rCBF (ml/min/gm) and V_f (vol/vol) is the effective fraction of capillary blood involved in the blood-to-brain transfer process [3]. From this relationship it follows that when K/FV_f is less than 0.1, K approximates PS with an error less than 6%. This situation obtains for normal gray and white matter structures ($10^{-2} > K_1 > 10^{-3}$ and $FV_f > 10^{-1}$) and for some primary and metastatic tumors [5, 18]. Dexamethasone has been shown to reduce rCBF in human brain tumors [24], but the magnitude of this decrease (10 to 14%) is unlikely to significantly affect the relationship between PS and K_1 in steroid-treated patients.

Effect of Corticosteroids

The first in vivo evidence that corticosteroids affect the blood-to-brain transport of low-molecular-weight tracers was provided by Marty and Cain [26], who described "improvement" in the follow-up technetium 99m ($^{99\text{m}}\text{Tc}$) brain scans of 7 of 10 brain tumor patients treated with pharmacological doses of dexamethasone. They postulated that the decreased uptake of tracer and associated clinical improvement were related to a steroid-induced reduction in peritumoral ECF volume. Crocker and associates [8] studied the effect of

steroids on the extravascular distribution of radiographic contrast material (iothalamate) and $^{99\text{m}}\text{Tc}$ pertechnetate using CT and emission CT. In 5 patients with brain tumors treated with dexamethasone (16 mg/day) they documented a reduction in tracer uptake and/or CT contrast enhancement—within 24 hours in one instance. The boundaries of contrast enhancement or $^{99\text{m}}\text{Tc}$ pertechnetate distribution were not altered by steroid therapy, and Crocker's group observed that iothalamate and pertechnetate uptake were reduced "irrespective of the presence of significant edema on CT scanning." They concluded that steroids decrease the permeability of brain tumor capillaries to CT and emission CT tracers.

Reverse transport of Rb from brain extracellular space into endothelial cell cytoplasm by $(\text{Na}^+ + \text{K}^+)\text{-ATPase}$ has been demonstrated [2, 9, 10], and steroids have been shown to inhibit the uptake of Rb by—but not the efflux of Rb from—isolated rat brain capillaries [7]. Although it is possible that steroids interact with endothelial cell $(\text{Na}^+ + \text{K}^+)\text{-ATPase}$ or other transport carriers to decrease Rb uptake into brain tumors, an effect on carrier transport mechanisms cannot adequately explain the decrease in brain/tumor capillary permeability to $^{99\text{m}}\text{Tc}$ pertechnetate, CT contrast agents, methotrexate, or serum albumin observed after corticosteroid administration [8, 14, 28, 29, 36, 39]. The effect of dexamethasone on V_p is interesting in view of a recent report that steroids decrease brain tumor extracellular space [28].

The data presented in Table 2 are consistent with the observed reduction in CT contrast enhancement of inflammatory and neoplastic brain lesions following corticosteroid therapy. If, as seems likely, corticosteroids produce a nonspecific decrease in BBB permeability to small polar molecules rather than a specific decrease in permeability to Rb or potassium, then steroid pretreatment may decrease the uptake of water-soluble chemotherapeutic agents into human brain tumors following intravenous or intracarotid administration. How the dexamethasone-induced reduction in tumor K_1 that we observed in 8 of 9 pre- and posttreatment ^{82}Rb /PET studies relates to the well-known anti-edema effect of corticosteroids remains to be established. In our small series of patients with brain tumors, moderate to marked clinical improvement was noted within 24 hours after the start of dexamethasone treatment. We can only speculate about the extent to which changes in tumor capillary permeability, $(\text{Na}^+ + \text{K}^+)\text{-ATPase}$ activity, and/or tumor ECF volume may contribute to this clinical improvement.

Effect of Radiation Therapy

The effect of radiation therapy on brain capillary permeability has been recognized for more than fifty years. Beclere [1], discussing the treatment of cranio-

spinal tumors, cautioned against the dangers of acute vasodilation, hyperemia, transudation of serous fluid, and edematous swelling. Hsu and associates [17] irradiated the heads of "deteriorated schizophrenic patients" and performed lumbar puncture 2.5 to 10.5 weeks after exposure to approximately 400% of the skin erythema dose; blood samples were obtained at the time of lumbar puncture, and both fluids were analyzed for bromides, chlorides, and sugar. Hsu's group reported a drop in the "bromide quotient" (bromides in blood/bromides in cerebrospinal fluid [CSF]) and "a rise of ratios of distribution of chlorides and sugar, implying an increase of permeability between blood and cerebrospinal fluid." These changes appeared in paired blood and CSF samples taken 4.5 and 6.5 weeks after irradiation.

Recent studies of the effect of cranial irradiation on BBB permeability to methotrexate in patients with leukemia-lymphoma have yielded conflicting results. Oliff and associates [31] described 5 pediatric patients who experienced severe encephalopathy within hours after receiving their initial 50- to 200-rad dose of cranial irradiation for the treatment of meningeal leukemia. Each patient had active meningeal disease at the time of treatment, and each had received one or more prior injections of intrathecal methotrexate. Oliff's group hypothesized that BBB alterations produced by the combination of intrathecal chemotherapy and cranial irradiation were responsible for the observed encephalopathy. In another study, Seshadri and colleagues [37] were unable to demonstrate an increase in the CSF/plasma ratio for methotrexate following cranial irradiation in 14 patients with acute leukemia-lymphoma. All patients were studied within 48 hours of completing a fractionated course of 2400-rad WBRT and within 3 hours after receiving an oral dose of methotrexate. In 6 of 8 patients with documented central nervous system disease, BBB permeability, as assessed by the CSF/plasma ratio for methotrexate, actually decreased.

Fike and co-workers [11] studied the effects of large single doses of x-irradiation on the normal canine brain using transmission CT and intravenously administered iodinated contrast material. They noted increasing contrast enhancement in the cerebellum, cerebrum, and midbrain beginning weeks to months after whole-brain irradiation, which they attributed to radiation-induced disturbances of the BBB. Levin and associates [25] investigated the acute effects of x-irradiation on brain capillary permeability in rats. In animals receiving single whole-brain doses of 200 or 400 rad, the permeability coefficient for galactitol, a small hydrophilic molecule (molecular weight, 182 daltons), increased more than 50% within 3 to 8 hours after irradiation. Thus, even low-dose cranial irradiation may acutely increase BBB permeability to hydrophilic molecules,

the transcapillary transport of which is normally highly restricted. Although the mechanism of this radiation effect has not been elucidated, selective biophysical damage to endothelial cell membranes [25] or opening of interendothelial tight junctions [32] would provide an explanation for the observed phenomena.

Corticosteroids protect against or moderate the acute complications of WBRT, and all of our patients undergoing WBRT were taking dexamethasone (4 to 16 mg/day) at the time of study. Thus, our failure to demonstrate an increase in blood-to-brain or blood-to-tumor transport of ^{82}Rb following WBRT may reflect the stabilizing effect of high-dose corticosteroids on the blood brain/tumor barrier.

Conclusions

The major advantage of our ^{82}Rb /PET method is the ability to obtain quantitative regional information about BBB function from a single 7-minute study. The regional PS product for Rb can be calculated if rCBF and V_f are known (see Equation 4).

Using ^{82}Rb /PET methods, it is now possible to define a dose-response curve for the anti-edema effect of dexamethasone and other potent corticosteroids and to determine the optimal steroid dose for individual patients with steroid-responsive neurological or neurosurgical diseases. For steroid-dependent patients with brain tumors undergoing systemic or intraarterial chemotherapy, ^{82}Rb /PET data can be used to design treatment protocols that maximize the delivery of tumoricidal drugs. Our data provide no support for the hypothesis that cranial irradiation enhances the toxicity of systemically administered drugs in the absence of subarachnoid metastases.

Supported in part by grant NS-15665 from the National Institute of Neurological and Communicative Disorders and Stroke.

The authors wish to thank Anastasia Gari for aid in data gathering and analysis, Mark Mernyk for invaluable electronics support, Dr Howard Thaler for biostatistical support, and Adele Ahronheim for manuscript preparation.

References

1. Beclere A: Les dangers a eviter dans la radiotherapie des tumeurs de la cavite cranio-rachidienne. *J Radiol* 10:556-563, 1926
2. Betz AL, Firth JA, Goldstein GW: Polarity of the blood brain barrier: distribution of enzymes between the luminal and antiluminal membranes of brain capillary endothelial cells. *Brain Res* 192:17-28, 1980
3. Blasberg RG, Fenstermacher JD, Patlak CS: Transport of alpha-aminoisobutyric acid across brain capillary and cellular membranes. *J Cereb Blood Flow Metab* 3:8-32, 1983
4. Blasberg RG, Wright DC, Patlak CS, et al: Determination of regional blood-tissue transfer constants and initial (plasma) volume in brain tumors using Ga-68-EDTA and dynamic positron emission tomography. *J Nucl Med* 25:P51, 1984

5. Brooks DJ, Beaney RP, Lammertsma AA, et al: Quantitative measurement of blood-brain barrier permeability using rubidium-82 and positron emission tomography. *J Cereb Blood Flow Metab* 4:535-545, 1984
6. Caveness WF: Experimental observations: delayed necrosis in normal monkey brain. In Gilbert HA, Kagan AR (eds): *Radiation Damage to the Nervous System, a Delayed Therapeutic Hazard*. New York, Raven, 1980
7. Chaplin ER, Free RG, Goldstein GW: Inhibition by steroids of the uptake of potassium by capillaries isolated from rat brain. *Biochem Pharmacol* 30:241-245, 1981
8. Crocker EF, Zimmerman RA, Phelps ME, Kuhl DE: The effects of steroids on the extravascular distribution of radiographic contrast material and technetium pertechnetate in brain tumors as determined by computed tomography. *Radiology* 119:471-474, 1976
9. Eisenberg HM, Suddith RL: Cerebral vessels have the capacity to transport sodium and potassium. *Science* 206:1083-1085, 1979
10. Eisenberg HM, Suddith RL, Crawford JS: Transport of sodium and potassium across the blood brain barrier. *Adv Exp Med Biol* 131:57-67, 1980
11. Fike JR, Cann CE, Davis RL, Phillips TL: Radiation effects in the canine brain evaluated by quantitative computed tomography. *Radiology* 144:603-608, 1982
12. Gennaro GP, Neirinckx RD, Bergner B, et al: A radionuclide generator and infusion system for pharmaceutical quality Rb-82. In Knapp FF Jr, Butler TA (eds): *Radionuclide Generators: New Systems for Nuclear Medicine Applications* (ACS Symposium Series No. 241). Washington, DC, American Chemical Society, 1984
13. Groothuis DR, Vriesendorp F, Mikhael M, et al: Quantitative measurement of brain tumor capillary permeability by CT: application in canine gliomas and implications for use in patients. *Neurology (Cleveland)* 34(suppl 1):185-186, 1984
14. Hatam A, Bergstrom M, Yu Z-Y, et al: Effect of dexamethasone treatment on volume and contrast enhancement of intracranial neoplasms. *J Comput Assist Tomogr* 7:295-300, 1983
15. Hawkins RA, Phelps ME, Huang S-C, et al: A kinetic evaluation of blood-brain barrier permeability in human brain tumors with [⁶⁸Ga]EDTA and positron computed tomography. *J Cereb Blood Flow Metab* 4:507-515, 1984
16. Hertz L: An intense potassium uptake into astrocytes, its further enhancement by high concentrations of potassium, and its possible involvement in potassium homeostasis at the cellular level. *Brain Res* 145:202-208, 1978
17. Hsu YK, Chang CP, Hsieh CK, Lyman RS: Effect of roentgen rays on the permeability of the barrier between blood and cerebrospinal fluid. *Chin J Physiol* 10:379-390, 1936
18. Ito M, Lammertsma AA, Wise RJS, et al: Measurement of regional cerebral blood flow and oxygen utilisation in patients with cerebral tumours using ¹⁵O and positron emission tomography: analytical techniques and preliminary results. *Neuroradiology* 23:63-74, 1982
19. Kearfott KJ: Radiation absorbed dose estimates for positron emission tomography (PET): K-38, Rb-81, Rb-82, and Cs-130. *J Nucl Med* 23:1128-1132, 1982
20. Kearfott KJ, Carroll LR: Evaluation of the performance characteristics of the PC 4600 positron emission tomograph. *J Comput Assist Tomogr* 8:502-513, 1984
21. Kearfott KJ, Rottenberg DA, Knowles RJR: A new headholder for PET, CT and NMR imaging. *J Comput Assist Tomogr* 8:1217-1220, 1984
22. Kessler RM, Goble JC, Bird JH, et al: Measurement of blood-brain barrier permeability with positron emission tomography and [⁶⁸Ga]EDTA. *J Cereb Blood Flow Metab* 4:323-328, 1984
23. Lammertsma AA, Brooks DJ, Frackowiak RSJ, et al: A method to quantitate the fractional extraction of rubidium-82 across the blood-brain barrier using positron emission tomography. *J Cereb Blood Flow Metab* 4:523-534, 1984
24. Leenders KL, Beaney RP, Brooks DJ: Dexamethasone effects in brain tumor patients measured with positron emission tomography. *Neurology (Cleveland)* 34(suppl 1):118, 1984
25. Levin VA, Edwards MS, Byrd A: Quantitative observations of the acute effects of X-irradiation on brain capillary permeability: Part I. *Int J Radiat Oncol Biol Phys* 5:1627-1631, 1979
26. Marty R, Cain ML: Effects of corticosteroid (dexamethasone) administration on the brain scan. *Radiology* 107:117-121, 1973
27. Mazziotta JC, Phelps ME, Plummer D, Kuhl DE: Quantitation in positron emission computed tomography: 5. Physical-anatomical effects. *J Comput Assist Tomogr* 5:734-743, 1981
28. Nakagawa H, Groothuis DR, Patlak CS, Blasberg RG: Dexamethasone reduces brain tumor extracellular space and capillary permeability: implications for diagnosis and therapy. *Neurology (Cleveland)* 34 (suppl 1):184, 1984
29. Neuwelt EA, Barnett PA, Bigner DD, Frenkel EP: Effects of adrenal cortical steroids and osmotic blood brain barrier opening on methotrexate delivery to gliomas in the rodent: the factor of the blood-brain barrier. *Proc Natl Acad Sci USA* 79:4420-4423, 1982
30. Nichols G Jr, Nichols N: Electrolyte equilibria in erythrocytes during diabetic acidosis. *J Clin Invest* 32:113-120, 1953
31. Oliff A, Bleyer WA, Poplack DG: Acute encephalopathy after initiation of cranial irradiation for meningeal leukaemia. *Lancet* 2:13-15, 1978
32. Olsson Y, Klatzo I, Carsten A: The effect of acute radiation injury on the permeability and ultrastructure of intracerebral capillaries. *Neuropathol Appl Neurobiol* 1:59-68, 1975
33. Reivich M, Jehle J, Sokoloff L, Kety SS: Measurement of regional cerebral blood flow with antipyrine-¹⁴C in awake cats. *J Appl Physiol* 27:296-300, 1969
34. Rottenberg DA, Chernik NL, Deck MDF, et al: Cerebral necrosis following radiotherapy of extracranial neoplasms. *Ann Neurol* 1:339-357, 1977
35. Rottenberg DA, Ginos JZ, Kearfott KJ, et al: In vivo measurement of brain tumor pH using [¹¹C]DMO and positron emission tomography. *Ann Neurol* 17:70-79, 1985
36. Sears ES, Tindall RSA, Zarnow H: Active multiple sclerosis: enhanced computerized tomographic imaging of lesions and the effect of corticosteroids. *Arch Neurol* 35:426-434, 1978
37. Seshadri RS, Ryall RG, Rice MS, et al: The effect of cranial irradiation on blood-brain barrier permeability to methotrexate. *Aust Paediatr J* 15:184-186, 1979
38. Sheppard CW, Martin WR: Cation exchange between cells and plasma of mammalian blood. I. Methods and application to potassium exchange in human blood. *J Gen Physiol* 33:703-722, 1950
39. Troiano R, Hafstein M, Ruderman M, et al: Effect of high-dose intravenous steroid administration on contrast-enhancing computed tomographic scan lesions in multiple sclerosis. *Ann Neurol* 15:257-263, 1984
40. Yano Y, Cahoon JL, Budinger TF: A precision flow-controlled Rb-82 generator for bolus or constant-infusion studies of the heart and brain. *J Nucl Med* 22:1006-1010, 1981
41. Yen CK, Budinger TF: Evaluation of blood brain barrier permeability changes in rhesus monkeys and man using Rb-82 and positron emission tomography. *J Comput Assist Tomogr* 5: 792-799, 1981
42. Yen CK, Yano Y, Budinger TF, et al: Brain tumor evaluation using Rb-82 and positron emission tomography. *J Nucl Med* 23:532-537, 1982
43. Young DF, Posner JB, Chu F, Nisce L: Rapid-course radiation therapy of cerebral metastases: results and complications. *Cancer* 34:1069-1076, 1974

44. Zipser A, Pinto HB, Fredberg AS: Distribution and turnover of administered rubidium (Rb 86) carbonate in blood and urine of man. *Appl Physiol* 5:317-322, 1953

Appendix

Model Considerations

In our two-compartment model, the brain/tumor compartment does not distinguish between extracellular and intracellular rubidium (Rb). The addition of a third compartment—intracellular Rb—and its uptake rate constant (k_3) would affect our estimates of the influx rate constant (K_1) as follows: If k_3 were small relative to K_1 and the efflux rate constant (k_2), incorporating k_3 into the model equation would result in a small increase in calculated extravascular brain activity but would produce no noticeable change in the estimates of K_1 and plasma water volume (V_p). If, on the other hand, k_3 were large relative to K_1 and k_2 , the effective K_1 calculated using Equation 3 would reflect both blood-brain barrier transport and cellular uptake of ^{82}Rb .

Linearized Approximation of Equation 3

When instantaneous brain activity is obtained from integrated brain activity by means of the approximation $A_m(t) = \int_0^T A_m(t) dt / T$, where T is the scan duration, Equation 3 takes the form

$$A_m(t) = \frac{V_p}{1 + k_2 t} C_p(t) + \frac{K_1 + k_2 V_p}{1 + k_2 t} \int_0^t C_p(u) du \quad \text{Eq A1}$$

where $A_m(t)$ is the ^{82}Rb concentration in brain tissue ($\mu\text{Ci}/\text{gm}$) and $C_p(t)$ is the instantaneous plasma ^{82}Rb concentration ($\mu\text{Ci}/\text{ml}$). For the special case when $k_2 = 0$ (no back flux),

$$A_m(t) + V_p C_p(t) + k_1 \int_0^t C_p(t) dt \quad \text{Eq A2}$$

If instantaneous brain activity can be obtained directly or indirectly from the positron emission tomographic (PET) scanner, Equation A1 allows for a multiple linear-regression approach to parameter estimation instead of the more sophisticated and time-consuming nonlinear least-squares regression required for the solution of Equation 3. For given coefficients of variation, model parameters can be estimated using Equation A1 (based on instantaneous brain activity) or Equation 3 (based on integrated brain activity) with the same degree of accuracy.

Error Analysis

In order to describe the uncertainty associated with model parameter estimates, computer simulations were carried out for both bolus-injection and constant-infusion (CI) protocols. The range of parameters selected for error analysis was: $0.0001 < K_1 < 0.1 \text{ ml}/\text{min}/\text{gm}$ and $0.03 < V_p < 0.08 \text{ ml}/\text{gm}$. k_2 was assumed to be equal to K_1 , and values for $C_p(t)$ were obtained from simulated blood radioactivity curves (adjusted for equal amounts of injected ^{82}Rb activity for bolus and CI protocols). Integrated brain activity was calculated at 1-minute intervals using Equation 3 and the above-mentioned system parameters. Gaussian noise (5 to 10%) was added to

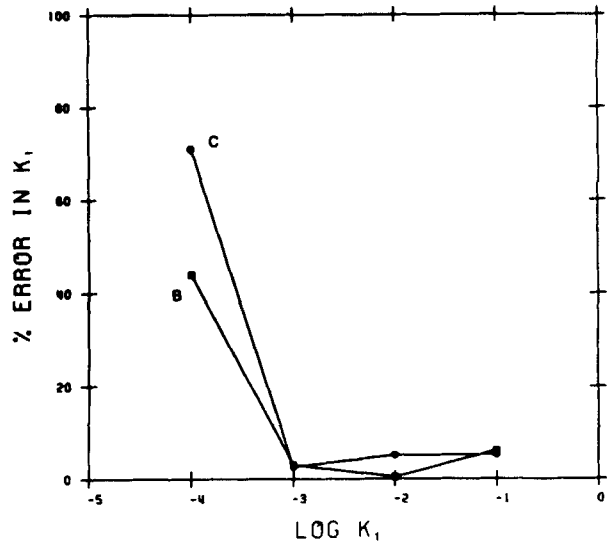


Fig 6. Percent error in \hat{K}_1 (absolute magnitude) as a function of the influx rate constant (K_1) for bolus-injection (B) and constant-infusion (C) protocols. The efflux rate constant (k_2) equals K_1 ; the tissue plasma water volume is 0.03; the error in brain tissue concentration (A_m) is assumed to be 5%. The instantaneous plasma ^{82}Rb concentration [$C_p(t)$] was derived from simulated blood radioactivity curves (see Appendix).

calculated regional brain activity. Error in $C_p(t)$ was neglected because blood radioactivity can usually be measured with high precision. Equation 3 was then solved for K_1 , k_2 , and V_p using a nonlinear regression routine, and the estimates thus obtained were compared with the actual parameters.

For the bolus injection technique, the error in \hat{K}_1 is less than 5% for $0.001 < K_1 < 0.1$ when V_p is 0.03 and the error in A_m (regional brain ^{82}Rb concentration as measured by PET) is 5%. The error in \hat{K}_1 increases sharply when K_1 is < 0.001 , exceeding 40% as K_1 approaches 0.0001. Increasing V_p to 0.08 increases the error in \hat{K}_1 only marginally.

For a 10% error in A_m and V_p of 0.03, the error in \hat{K}_1 is less than 13% for $0.001 < K_1 < 0.1$. However, if V_p is 0.08, the error in \hat{K}_1 ranges from 35 to 1% for $0.01 < K_1 < 0.1$. The error in \hat{V}_p is less than 6% over the whole range of K_1 . k_2 is associated with very large errors ($> 70\%$) when K_1 is < 0.01 , V_p is > 0.03 , and the error in A_m is $> 5\%$.

For the CI protocol, errors in \hat{K}_1 are similar to those projected for the bolus-injection case except when K_1 is < 0.001 (Fig 6). The CI technique, however, is more sensitive to changes in V_p and to errors in PET measurement of brain activity than is the bolus technique.

When k_2 is zero, Equation 3 reduces to the integrated form of Equation 2. For both bolus and CI protocols, we carried out simulations in which k_2 was set equal to zero: The error in derived estimates in K_1 was greater with a k_2 of zero than with $K_1/10 < k_2 < K_1 \cdot 10$. Thus, the very inclusion of k_2 —though k_2 was associated with large errors for $k_2 < 0.05$ —improved our estimates of K_1 .